Supplementary Materials

1. Tables

Table S1 List of the information of antibodies.

Antibody	Dilutions	Source	Cat. no.
VDAC1	1:1000 (IB)	Millipore	MABN504A
VDAC2	1:1000 (IB)	Thermo Fisher Scientific	PA1-958
VDAC3	1:2000 (IB)	Proteintech	55260-1-AP
COX4	1:1000 (IB)	Cell Signaling Technology	4844
p53	1:1000 (IB)	Santa Cruz	Sc-126
	1:500 (IF)		
p-CREB (Ser133)	1:200 (IF)	Abcam	ab32096
CDK9	1:1000 (IB)	Santa Cruz	Sc-13130
	1:100 (IF)		
p-CDK9 (Thr186)	1:1000 (IB)	Affinity Biosciences	AF4440
	1:100 (IF)		
β-actin	1:10000 (IB)	Cell Signaling Technology	3700
α-tubulin	1:50000 (IB)	Proteintech	66031-1-Ig
Anti-mouse lgG	1:10000 (IB)	Cell Signaling Technology	7076
Anti-rabbit lgG	1:10000 (IB)	Cell Signaling Technology	7074
Anti-chicken IgY	1:10000 (IB)	Thermo Fisher Scientific	SA1-9509
NeuN	1:2000 (IF)	Cell Signaling Technology	12943
Alexa Fluor 568 goat anti-mouse IgG	1:500 (IF)	Invitrogen	A11004
Alexa Fluor 488 goat anti-rabbit IgG	1:500 (IF)	Invitrogen	A11070

Table S2 List of primer sequences for quantitative PCR.

Target genes	Direction	Primer sequence (5' to 3')
Hk1	Forward	GAAGCGAGGGGACTATGACG
	Reverse	ATCAGGCCGACTTCACACTG
Pfk1	Forward	TGCAGACTGCTTGATTCGGT
	Reverse	TTGGAGCTGATGGAAGGCAG
Ldha	Forward	CAAGGAGCAGTGGAAGGAGG
	Reverse	CCAAGTCTGCCACAGAGAGG
G6pd	Forward	GTGCTGAGGTTTGCCAACAG
	Reverse	TCAAAATAGCCCCCACGACC
Vdac1	Forward	ACTGAGAGCGAGACCCCATA
	Reverse	ACAGTTGCATTTGGCGACAC
Vdac2	Forward	GGGGACTTCCAGCTACACAC
	Reverse	ACGAGTGCAGTTGGTACCTG
Vdac3	Forward	TTGCGACCTAGGAAAGGCTG
	Reverse	TTCCATCACTCCACTACAAGAC
Trp53	Forward	CCATGGCCCCTGTCATCTTT
	Reverse	TGAGGGGAGGAGAGTACGTG
β-actin	Forward	ACTGTCGAGTCGCGTCCA
	Reverse	GTCATCCATGGCGAACTGGT
pri-miR-183/96/182	Forward	CCAGGAGAAGGCAGCTGA
	Reverse	AGGCAGAAAGGGGTGAGGA
miR-183	RT primer	GTCGTATCCAGTGCAGGGTCCGAGGTATTCG
		CACTGGATACGACAGTGAAT
	Forward	CTGGAGTATGGCACTGGTAGAA
	Reverse	GTGCAGGGTCCGAGGT

miR-96	RT primer	GTCGTATCCAGTGCAGGGTCCGAGGTATTCG
		CACTGGATACGACAGCAAAA
	Forward	CTGGAGTTTGGCACTAGCACAT
	Reverse	GTGCAGGGTCCGAGGT
miR-182	RT primer	GTCGTATCCAGTGCAGGGTCCGAGGTATTCG
		CACTGGATACGACCGGTGTG
	Forward	CTGGAGTTTGGCAATGGTAGAA
	Reverse	GTGCAGGGTCCGAGGT
U6	RT primer	AAAATATGGAACGCTTCACGAATTTG
	Forward	CTCGCTTCGGCAGCACATATACT
	Reverse	ACGCTTCACGAATTTGCGTGTC

Table S3 List of sequences of miRNA mimics.

miRNA mimic	**Sequence (5' to 3')**
miR-183 mimic	UAUGGCACUGGUAGAAUUCACU
miR-96 mimic	UUUGGCACUAGCACAUUUUUGCU
miR-182 mimic	UUUGGCAAUGGUAGAACUCACACCG
miR-NC	UUCUCCGAACGUGUCACGUTT

2. Figures

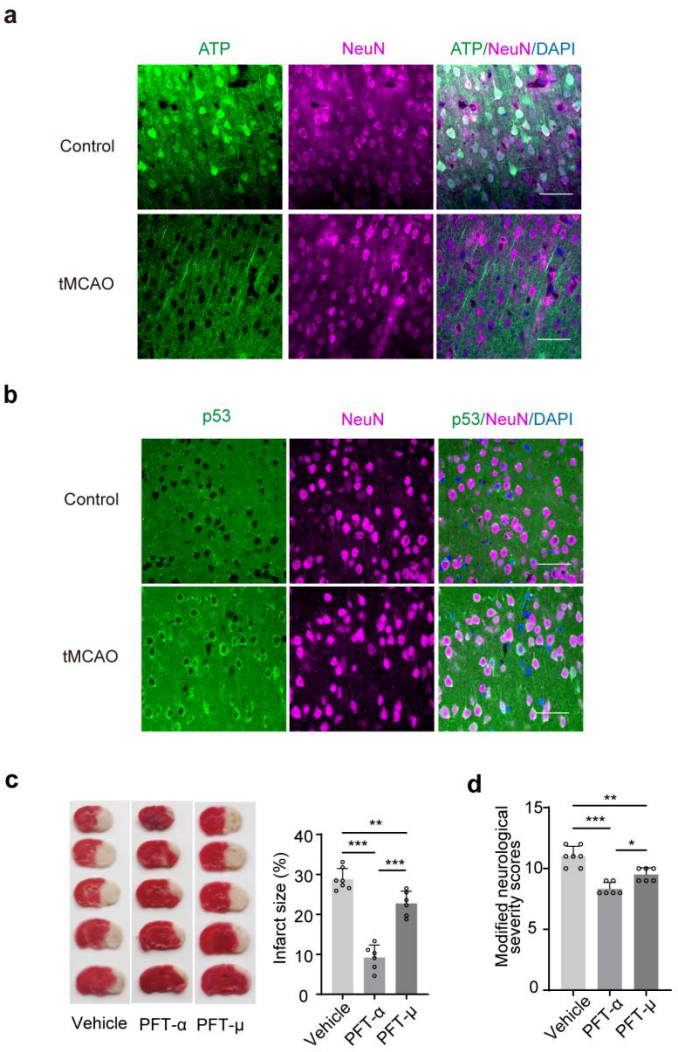

Fig. S1 p53 transcriptional activity drives ATP decline and neural impairments after AIS.

(**a**) Fluorescent imaging of ATP levels within neurons in the peri-infarct region of the tMCAO and contralateral cortexes (control) 24 h after reperfusion. Co-staining with NeuN marks neurons (including 15 slices from three mice). Scale bar = 50 μm. (**b**) IF staining for p53 expression in the peri-infarct region of the tMCAO cortex and its contralateral cortex (control) 6 h after reperfusion. Co-staining with NeuN marks neurons (including 15 slices from three mice). Scale bar = 50 μm. (**c** and **d**) TTC analysis and quantification of cerebral infarct size (**c**), and mNSS assessment for neurological deficits (**d**) in mice treated with vehicle, PFT-α, or PFT-μ 48 h after reperfusion (n = 6 or 7). Data are shown as the mean ± SD and were analyzed using one-way ANOVA. *P < 0.05; **P < 0.01; ***P < 0.001.

Fig.S2

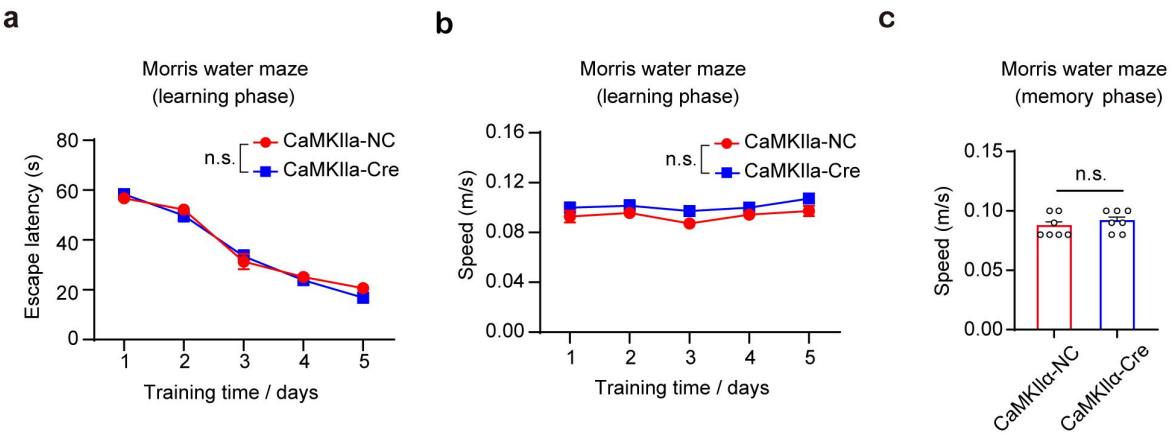

Fig. S2 The conditional deletion of neuronal p53 does not impact learning ability in mice after AIS.

(**a-b**) Morris water maze test showing escape latency (**a**) and swimming speed (**b**) in mice subjected to five sessions of training after tMCAO (one session per day). Data are shown as the mean ± SEM and were analyzed using two-way ANOVA with repeated measures. n.s., not significant. (**c**) Morris water maze test showing swimming speed in mice in the memory phase after tMCAO (n = 7). Data are shown as the mean ± SEM and were analyzed using unpaired t-tests. n.s., not significant.

Fig.S3

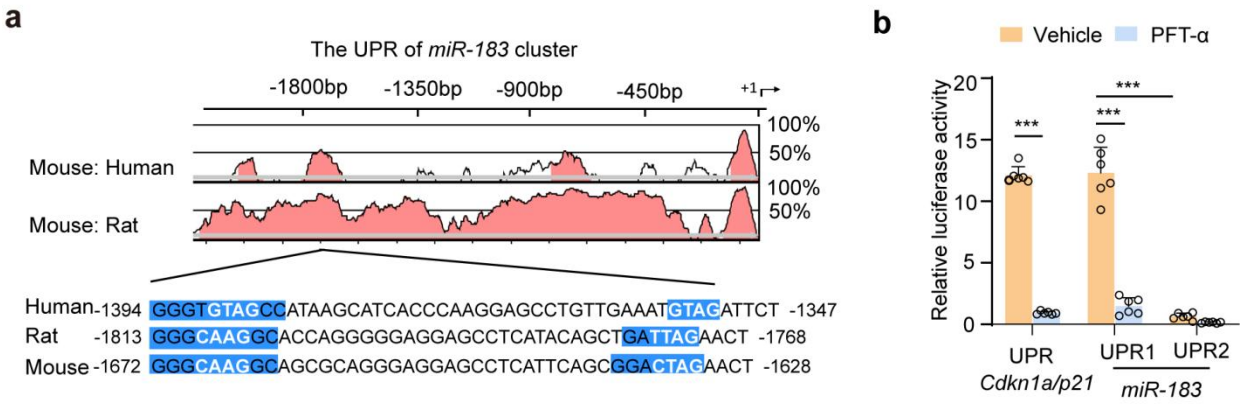

Fig. S3 Analysis of transcriptional regulation sequence of p53 with the *miR-183* cluster.

(**a**) Diagrammatic illustration of the pairwise comparison of the UPRs and PREs for p53 in the *miR-183* cluster among humans, rats, and mice using the VISTA website. (**b**) Dual-luciferase reporter assay of p53 *trans*-interaction with UPR1 (-3000 to -1600) or UPR2 (-1600 to -1) constructs of the *miR-183* cluster, which were transfected into HT22 neuronal cells treated with or without PFT-α (5 μM). Data are shown as the mean ± SD (n = 6, from at least three independent cultures) and were analyzed using two-way ANOVA. ***$P < 0.001$.

Fig.S4

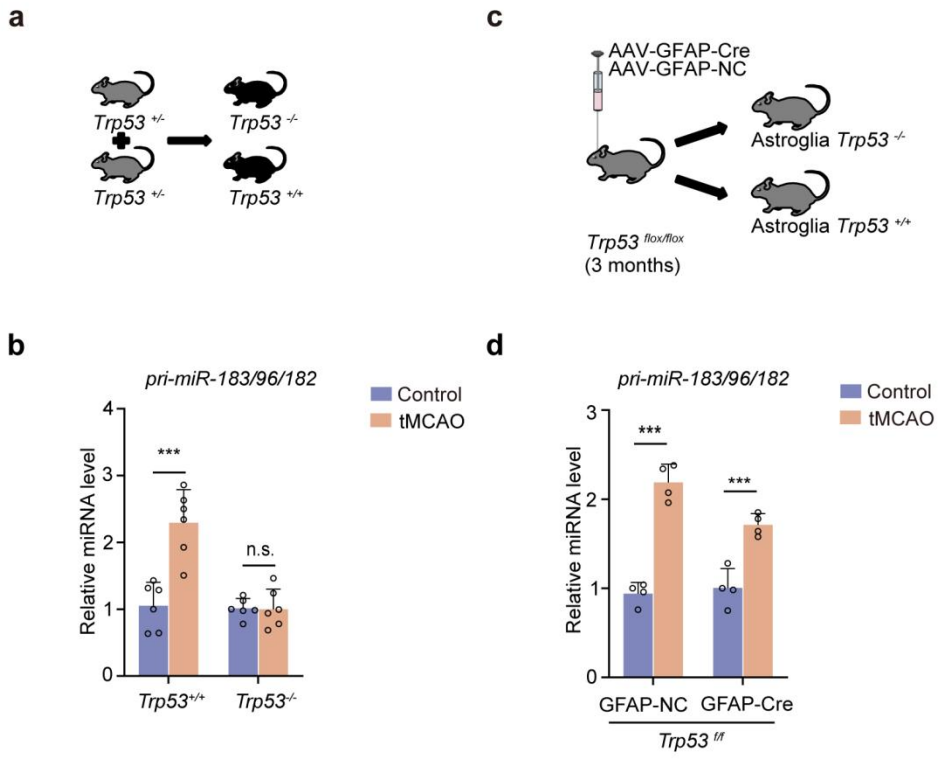

Fig. S4 Detection of the transcripts of the *miR-183* cluster in general p53 ablation and astroglia p53 ablation mice after tMCAO.

(**a**) Schematic protocol of the generation of *Trp53*$^{+/+}$ and *Trp53*$^{-/-}$ mice. (**b**) Relative *pri-miR-183/96/182* levels in the mouse peri-infract region of the tMCAO and contralateral control cortexes 3 h after reperfusion (qPCR; $n = 6$). (**c**) Schematic diagram showing specific knockout of p53 in astroglia through AAV-GFAP-Cre injection or its negative control (AAV-GFAP-NC) in *Trp53*$^{flox/flox}$ mice. (**d**) Relative *pri-miR-183/96/182* levels in astroglia p53 ablation mice 3 h after reperfusion (qPCR; $n = 4$). Data are shown as the mean ± SD and were analyzed using two-way ANOVA. ***$P < 0.001$; n.s., not significant.

Fig.S5

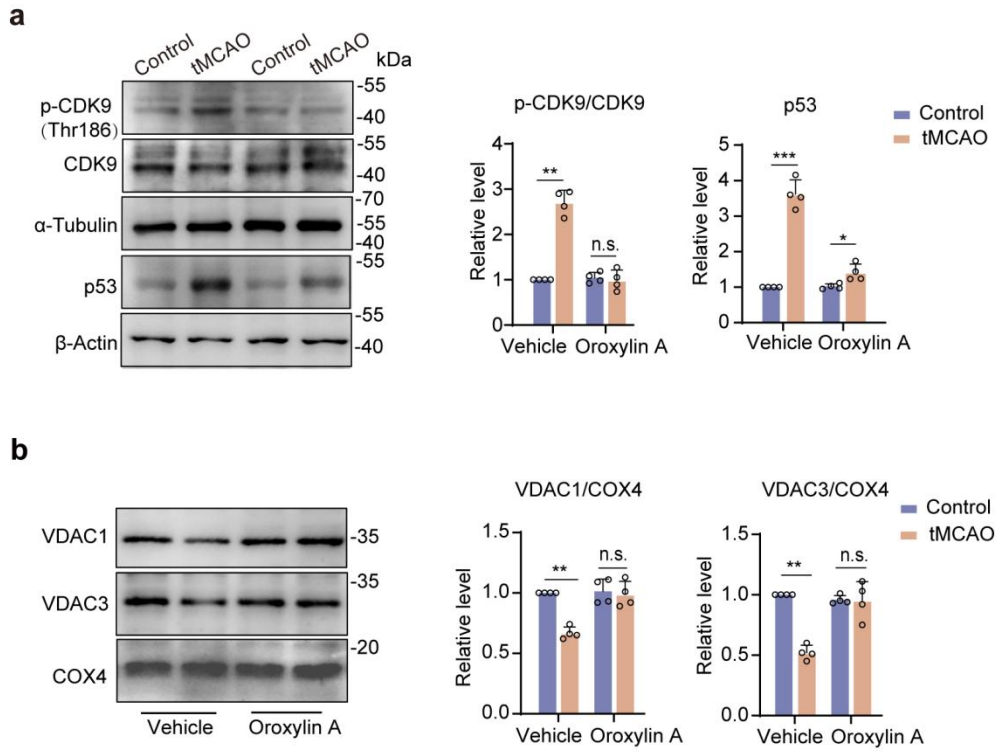

Fig. S5 Inhibition of CDK9 by oroxylin A mitigates the p53/VDACs signaling pathways in female mice after AIS.

(**a**) Immunoblotting assessment of CDK9 (phosphorylated and total protein) and p53 levels in female mice 24 h after reperfusion after treatment with vehicle or oroxylin A. Beta-Actin and α-Tubulin served as loading controls. (**b**) VDAC1 and VDAC3 levels 24 h after reperfusion in mice after treatment with vehicle or oroxylin A. COX4 served as the loading control. Data are shown as the mean ± SD (n = 4) and were analyzed using one-way ANOVA. *P < 0.05; **P < 0.01;***P < 0.001; n.s., not significant.

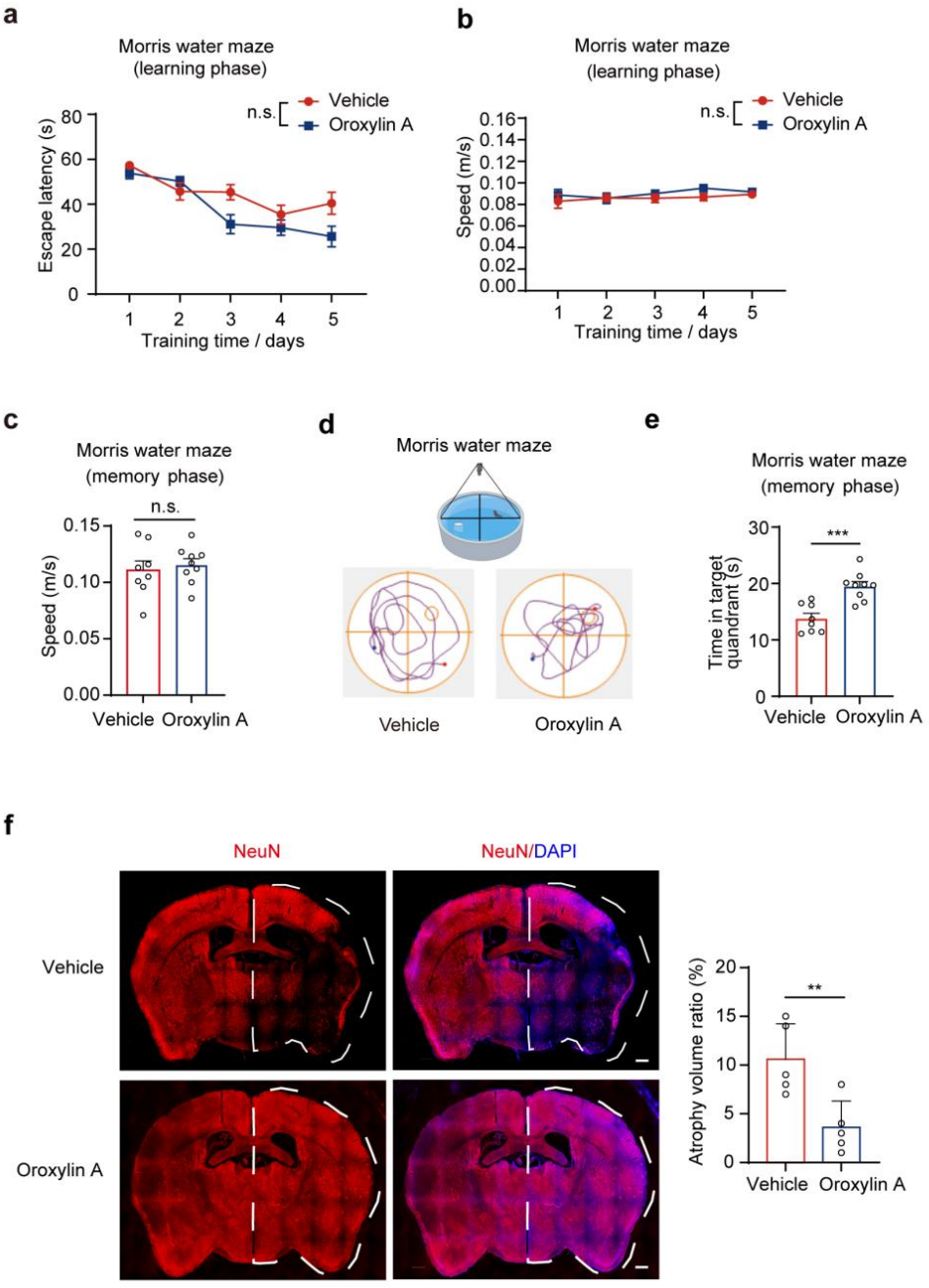

Fig. S6 Oroxylin A therapy has no effect on learning ability in mice after AIS, but it reduces chronic brain tissue loss after 33 days compared to the vehicle group.

(**a**-**b**) Morris water maze test showing escape latency (**a**) and swimming speed (**b**) in mice subjected to five sessions of training after tMCAO (one session per day). Data are shown as the mean ± SEM and were analyzed using two-way ANOVA with repeated measures (n = 8 vehicle, and n = 9 oroxylin A). n.s., not significant. (**c**) Morris

water maze test showing swimming speed in mice in the memory phase after tMCAO. (**d**-**e**) Analysis of the time in the target quadrant during the memory phase 29 days after reperfusion after tMCAO in the Morris water maze. Data are shown as the mean ± SEM and were analyzed using unpaired *t*-tests ($n = 8$ vehicle, and $n = 9$ oroxylin A). ***$P < 0.001$; n.s., not significant. (**f**) Representative images of IF staining for NeuN expression followed by quantitative comparison measured 33 days after tMCAO to evaluate brain tissue atrophy. Co-staining with DAPI (including 5 brain slices from five mice). Scale bar = 500 μm. Data are shown as the mean ± SD and were analyzed using unpaired *t*-tests. **$P < 0.01$.